Chemistry Faculty Publications

Chemistry

4-1998

Distance Dependence Of Electron Transfer Along Artificial Beta-strands At 298 And 77 K

S. R. L. Fernando

Gennady V. Kozlov

Michael Y. Ogawa
Bowling Green State University, mogawa@bgsu.edu

Distance Dependence of Electron Transfer along Artificial β-Strands at 298 and 77 K

S. R. L. Fernando, Gennady V. Kozlov, and Michael Y. Ogawa*

Department of Chemistry, Center for Photochemical Sciences, Bowling Green State University, Bowling Green, Ohio 43403

Photoinduced electron-transfer rate constants were measured for a series of binuclear metallopeptides consisting of a $[Ru(bpy)_2(cmbpy)]^{2+}$ electron donor tethered to a $Co^{III}(NH_3)_5$ electron acceptor by an oligovaline peptide chain (bpy = 2,2′-bipyridine, cmbpy = 4-carboxy-4′-methyl-2,2′-bipyridine). These compounds were shown by ^1H NMR to adopt the conformational properties found within the individual strands of a β-pleated sheet in both aqueous and methanol solutions. Emission lifetime measurements and HPLC product analysis show that the binuclear donor/acceptor compounds undergo photoinduced electron transfer (ET). The values of k_{et} decrease with increasing donor/acceptor distance according to the expression $k_{et} = k' \exp[-\beta(r - r_0)]$. A distance attenuation factor of $\beta = 1.1 \pm 0.4$ Å^{-1} is seen both in H_2O at 298 K and in an ethanol−methanol glass at 77 K. The ET kinetics obtained at 77 K for **1**−**3** were single exponential, indicating that the compounds maintain a unique donor/acceptor separation and do *not* exist within multiple conformations. The similarity in behavior obtained under very different solvent conditions indicates that the electronic coupling term dominates the distance dependence of k_{et}.

Introduction

Electron-transfer (ET) reactions comprise the fundamental steps of biochemical energy conversion. Because these reactions involve interactions between distantly located, protein-bound redox centers, efforts to understand their mechanisms have centered around the study of photosynthetic reaction centers,[1] surface-derivatized proteins,[2,3] protein−protein complexes,[4−7] and artificial polypeptides.[8−16]

Results from a large body of work have shown that the rates of nonadiabatic ET reactions can be described by eq 1 where

$$k_{et} = (4\pi^2/h)(\text{FCWD})|H_{DA}(r)|^2 \qquad (1)$$

FCWD is the Franck−Condon weighted density of states and $H_{DA}(r)$ is the electronic coupling matrix element.[17] In eq 1, the Franck−Condon term describes how ET rates are controlled by the interplay between the thermodynamic driving force ($\Delta G°$) and reorganization energy (λ) for the reaction. The electronic term, $H_{DA}(r)$, describes how these reactions result from the overlap between the appropriate donor and acceptor orbitals. Both of these terms contribute to the distance dependence of k_{et}.[18] Studies of rigidly linked donor/acceptor molecules have shown that H_{DA} generally obeys the functional form

$$H_{DA}(r) = H_0 \exp[-\beta(r - r_0)/2] \qquad (2)$$

where the distance attenuation factor (β) reflects the efficacy of coupling between the donor and acceptor sites, r is the donor/ acceptor distance, and r_0 is the sum of their van der Waals radii, usually taken to be 3 Å.[19−21] Thus, in situations where the

(1) *The Photosynthetic Reaction Center*; Deisenhofer, J., Norris, J. R., Eds.; Academic: New York, 1993.
(2) (a) Sun, J.; Wishart, J. F.; Gardineer, M. B.; Cho, M. P.; Isied, S. S. *Inorg. Chem.* **1995**, *34*, 3301. (b) Moreira, I.; Sun, J.; Cho, M. P.; Wishart, J. F.; Isied, S. S. *J. Am. Chem. Soc.* **1994**, *116*, 8396.
(3) Casimiro, D. R.; Beratan, D. N.; Onuchic, J. N.; Winkler, J. R.; Gray, H. B. in *Adv. Chem. Ser.* **1995**, *246*, 471.
(4) (a) Corin, A. F.; Hake, R. A.; McLendon, G.; Hazzard, J. T.; Tollin, G. *Biochemistry* **1993**, *32*, 2756. (b) Qiao, T.; Simmons, J.; Horn, D. A.; Chandler, R.; McLendon, G. *J. Phys. Chem.* **1993**, *97*, 13089.
(5) Zhou, J. S.; Hoffman, B. M. *Science* **1994**, *265*, 1693.
(6) Hahm, S.; Durham, B.; Millett, F. *Biochemistry* **1992**, *31*, 3472.
(7) Zhou, J. S.; Kostic, N. M. *J. Am. Chem. Soc.* **1992**, *114*, 3562.
(8) Gretchikhine, A. B.; Ogawa, M. Y. *J. Am. Chem. Soc.* **1996**, *118*, 1543.
(9) Kozlov, G. V.; Ogawa, M. Y. *J. Am. Chem. Soc.* **1997**, *119*, 8377.
(10) (a) Isied, S. S.; Ogawa, M. Y.; Wishart, J. F. *Chem. Rev.* **1993**, *92*, 381. (b) Ogawa, M. Y.; Wishart, J. F.; Young, Z.; Milller, J. R.; Isied, S. S. *J. Phys. Chem.* **1993**, *97*, 11456. (c) Ogawa, M. Y.; Moreira, I.; Wishart, J. F.; Isied, S. S. *Chem. Phys.* **1993**, *176*, 589.
(11) Mutz, M. W.; McLendon, G. L.; Wishart, J. F.; Gaillard, E. R.; Corin, A. F. *Proc. Natl. Acad. Sci. U.S.A.* **1996**, *93*, 9521.
(12) (a) Galoppini, E.; Fox, M. A. *J. Am. Chem. Soc.* **1996**, *118*, 2299. (b) Batchelder, T. L.; Fox, R. J., III; Meier, M. S.; Fox. M. A. *J. Org. Chem.* **1996**, *61*, 4206.
(13) Mecklenburg, S. L.; McCafferty, D. G.; Schoonover, J. R.; Peek, B. M.; Erickson, B. W.; Meyer, T. J. *Inorg. Chem.* **1994**, *33*, 2974.
(14) (a) DeFilippis, M. R.; Faraggi, M.; Klapper, M. H. *J. Am. Chem. Soc.* **1990**, *112*, 5640. (b) Faraggi, M.; DeFilippis, M. R.; Klapper, M. H. *J. Am. Chem. Soc.* **1989**, *111*, 5141.
(15) (a) Inai, Y.; Sisido, M.; Imanishi, Y. *J. Phys. Chem.* **1991**, *95*, 3847. (b) Inai, Y.; Sisido, M.; Imanishi, Y. *J. Phys. Chem.* **1990**, *94*, 6237. (c) Sisido, M.; Tanaka, R.; Inai, Y.; Imanishi, Y. *J. Am. Chem. Soc.* **1989**, *111*, 6790.
(16) Schanze, K. S.; Sauer, K. *J. Am. Chem. Soc.* **1988**, *110*, 1180.
(17) Marcus, R. A.; Sutin, N. *Biochim. Biophys. Acta* **1985**, *811*, 265.
(18) Isied, S. S.; Vassilian, A.; Wishart, J. F.; Creutz, C.; Schwarz, H. A.; Sutin, N. *J. Am. Chem. Soc.* **1988**, *110*, 635.
(19) Closs, G. L.; Calcaterra, L. T.; Green, N. J.; Penfield, K. W.; Miller, J. R. *J. Phys. Chem.* **1986**, *90*, 3673.
(20) (a) Paddon-Row, M. N.; Oliver, A. M.; Warman, J. M.; Smit, K. J.; de Haas, M. P.; Oevering, H.; Verhoeven, J. W. *J. Phys. Chem.* **1988**, *92*, 6958. (b) Oevering, H.; Paddon-Row, M. N.; Heppener, M.; Oliver, A. M.; Cotsaris, E.; Verhoeven, J. W.; Hush, N. S. *J. Am. Chem. Soc.* **1987**, *109*, 3258.
(21) Stein, C. A.; Lewis, N. A.; Seitz, G. *J. Am. Chem. Soc.* **1982**, *104*, 2596.
(22) (a) Moser, C. C.; Page, C. C.; Farid, R.; Dutton, P. L. *J. Bioenerg. Biomembr.* **1995**, *27*, 263. (b) Dutton, P. L.; Moser, C. C. *Proc. Natl. Acad. Sci. U.S.A.* **1994**, *91*, 10247. (c) Moser, C. C.; Keske, J. M.; Warncke, K.; Farid, R. S.; Dutton, P. L. *Nature* **1992**, *355*, 796.

electron transfer is dominated by H_{DA}, the magnitude of k_{et} is expected to decay exponentially with the donor/acceptor distance according to eq 3.

$$k_{et} = k' \exp[-\beta(r - r_0)] \qquad (3)$$

In recent years, an important discussion has developed concerning the role of the intervening protein matrix in mediating protein-based ET reactions. Dutton and co-workers[22] have made an extensive comparison of the biological ET data and note that the protein matrix can be largely modeled as a *homogeneous barrier* to electron tunneling where $\beta = 1.4$ Å^{-1}. In contrast, numerous studies of ruthenium-modified metalloproteins have shown that activationless ET rates do *not* always follow a simple exponential distance dependence.[23,24] Rather, in these systems it appears that the distance attenuation of k_{et} is largely determined by the number of covalent, hydrogen-bond, and through-space contacts which connect the donor and acceptor sites.[25] This apparent contradiction in the existing electron-transfer data shows that the mechanistic role of the intervening protein matrix is not easily understood.

To better understand the nature of biological ET reactions, we[8,9] and others[10−16] have begun to examine the ET properties of peptide-based model systems having well-defined secondary structures. Our group recently reported the ET properties of a metallopeptide-based mimic of a parallel β-pleated sheet.[8,26] β-Sheets are a common protein structure motif that consists of a two-dimensional array of fully extended polypeptide chains stabilized by a pattern of interchain hydrogen bonds. Each individual peptide chain of a β-sheet (i.e., a β-strand) is characterized by specific values for the peptide dihedral angles ϕ and ψ.[27] Here, we report the first study of the distance dependence of ET rates occurring within a small series of metallopeptides whose conformational properties are identical to those of the individual strands of a β-pleated sheet. These compounds have the general form [(bpy)$_2$Ru(cmbpy)−(Val)$_n$−Co(NH$_3$)$_5$]$^{4+}$, where bpy = 2,2′-bipyridine, cmbpy = 4-carboxy-4′-methyl-2,2′-bipyridine, Val = L-valine, and $n = 1−3$ (Figure 1).

Experimental Section.

General Methods. All chemicals and solvents were of reagent grade and were used as received without further purification. [Ru(bpy)$_3$]Cl$_2$ and [Ru(bpy)$_2$Cl$_2$] were purchased from Aldrich Chemicals. HPLC analyses were performed on a single-pump system (Waters model 510) equipped with a binary gradient controller (Autochrom. Inc.) and a Waters model 994 diode array detector/spectrophotometer. HPLC eluents consisted of helium-purged acetonitrile/water gradients (20−40% v/v) containing trifluoroacetic acid (0.1% v/v). UV/vis spectra were recorded on a Hewlett-Packard model 8452A diode array spectrophotometer.

¹H NMR Measurements. ¹H NMR spectra were recorded on a Varian Unityplus 400 spectrometer (400 MHz) in D$_2$O, D$_2$O/H$_2$O (10% v/v), or CD$_3$OH. Presaturation solvent suppression was used when
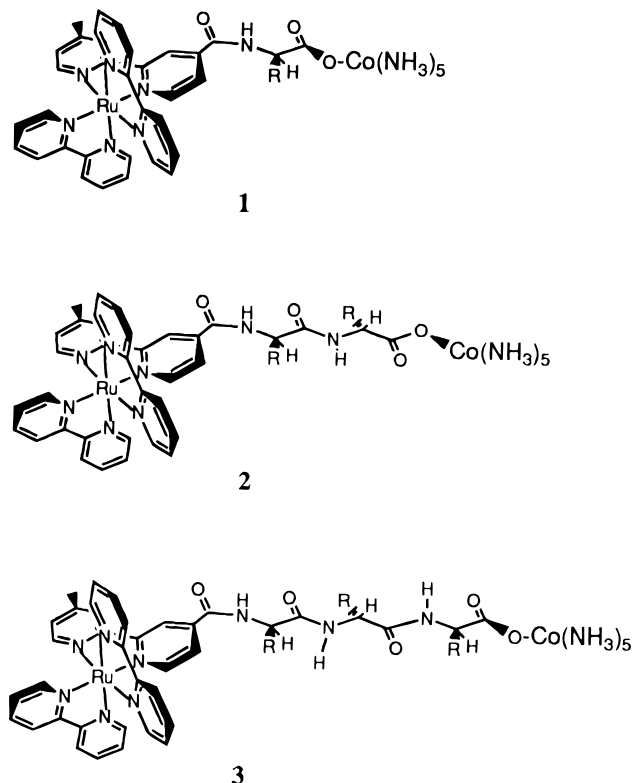

Figure 1. Binuclear metallopeptides having the conformational properties of single β-strands (**1−3**), R = −CH$_2$(CH$_3$)$_2$.

needed. Peak assignments were made on the basis of TOCSY, DQCOSY, and ROESY data. The free induction decays were multiplied by an exponential apodization function for both dimensions of the TOCSY and ROESY spectra. A shifted sine bell apodization was used for the DQCOSY data prior to Fourier transformation. Zero filling and linear prediction were used for the 2-D processing, and baseline correction was applied when needed. The experimental parameters such as mixing time, solvent suppression parameters, spin-lock power, offset frequency, saturation power, and number of transients were varied to optimize the intensity of the amide signals and maximize solvent suppression. DSS was used as an internal reference.

Molecular Modeling Studies. Molecular modeling studies were performed on a Silicon Graphics, Inc., Indy workstation using the Spartan software package (Wavefunction, Inc., Irvine, CA). The appropriate chemical structures were energy-minimized using the SYBYL molecular mechanics force field. The through-space donor−acceptor distances were measured from the edge of the cmbpy bipyridyl ring to the center of the cobalt atom.

Steady-State Emission Measurements. Steady-state emission spectra were recorded on a Spex Fluorolog fluorimeter equipped with two monochromators. The excitation wavelength was set at 458 nm. Corrections for detector sensitivity and background signals were performed for all spectra using the manufacturer's software routine.

Emission Lifetime Measurements. Emission lifetime measurements were obtained using a Q-switched Nd:YAG laser system (Continuum, YG660). Most experiments used either 355 or 532 nm output (ca. 7 ns pulse width) with a diverging lens placed before the sample to expand the incident beam. The emission at 640 or 600 nm was monitored using a computer-controlled kinetic spectrophotometer (Kinetic Instruments). Appropriate interference filters were placed before the entrance slit of monochromator to remove scattered light. Lifetime data and initial intensities of the emission decay curves were evaluated using PC RAD PROGRAM (Kinetic Instruments). All lifetime measurements were performed in argon-saturated solutions to avoid possible complications arising from the presence of either oxygen or carbon dioxide in solution.

(23) Bowler, B. E.; Raphael, A. L.; Gray, H. B. *Prog. Inorg. Chem.* **1990**, *38*, 259.

(24) (a) Casimiro, D. R.; Richards, J. H.; Winkler, J. R.; Gray, H. B. *J. Phys. Chem.* **1993**, *97*, 13073. (b) Casimiro, D. R.; Wong, L.-L.; Colon, J. L.; Zewert, T. E.; Richards, J. H.; Chang, I.-J.; Winkler, J. R.; Gray, H. B. *J. Am. Chem. Soc.* **1993**, *115*, 1485.

(25) (a) Curry, W. B.; Grabe, M. D.; Kurnikov, I. V.; Skourtis, S. S.; Beratan, D. N.; Regan, J. J.; Aquino, A. J.; Beroza, P.; Onuchic, J. N. *J. Bioenerg. Biomembr.* **1995**, *27*, 285. (b) Skourtis, S. S.; Regan, J. J.; Onuchic, J. N. *J. Phys. Chem.* **1994**, *98*, 3379. (c) Regan, J. J.; Risser, S. M.; Beratan, D. N.; Onuchic, J. N. *J. Phys. Chem.* **1993**, *97*, 13083.

(26) Ogawa, M. Y.; Gretchkhine, A. B.; Soni, S. D.; Davis, S. M. *Inorg. Chem.* **1995**, *34*, 6423.

(27) Wuthrich, K. *NMR of Proteins and Nucleic Acids*; John Wiley & Sons: New York, 1986.

Table 1. Emission and Electron Transfer Parameters of $[(bpy)_2Ru(cmbpy)(Val)_nCo(NH_3)_5]^{4+}$ in Water and 4:1 (v/v) Ethanol−Methanol

compd	$d_{D-A}{}^a$ (Å)	λ_{max} (nm) H₂O, 298 K	λ_{max} (nm) EtMe, 298 K	λ_{max} (nm) EtMe, 77 K	Φ_{em} H₂O, 298 K	τ (ns)^b H₂O,^{c} 298 K	τ (ns)^b EtMe, 298 K	τ (ns)^b EtMe, 77 K	k_{et} (s⁻¹) H₂O, 298 K	k_{et} (s⁻¹) EtMe, 298 K	k_{et} (s⁻¹) EtMe, 77 K
1	8.1	666	646	600, 645, ~710 (sh)	<0.0032^d	0.5 ± 0.3, 380 ± 10^e	<0.5, 1160 ± 20^e	10 ± 4, 4850 ± 100^e	2.0 × 10⁹	>2.0 × 10⁹	1.0 × 10⁸
1′		667	644	598, 645, ~710 (sh)	0.020	393 ± 8	1100 ± 50	5210 ± 100			
2	11.8	670	646	600, 645, ~710 (sh)	0.0087	123 ± 20, 373 ± 6^e	77 ± 8, 1070 ± 50^e	2620 ± 250	5.5 × 10⁶	1.2 × 10⁷	1.6 × 10⁵
2′		670	645	606, 649, ~710 (sh)	0.019	383 ± 6	1120 ± 40	4610 ± 400			
3	15.2	671	647	601, 646, ~710 (sh)	0.014	290 ± 12	220 ± 30, 1110 ± 50^e	4250 ± 300	7.2 × 10⁵	3.7 × 10⁶	4.4 × 10⁴
3′		671	647	602, 647, ~710 (sh)	0.019	366 ± 5	1140 ± 40	5230 ± 300			
Ru(bpy)₃²⁺		628	629	584, 633, 685	0.042	574	960 ± 20	4830 ± 100			

^{a} Obtained from computer modeling studies as described in the text. Distances are measured from the edge of the cmbpy ligand to the center of the cobalt atom. ^{b} The uncertainities listed for the lifetime data are standard deviations of measurements obtained from multiple samples. ^{c} Emission lifetimes are concentration independent within the range 5−50 μM in H₂O. ^{d} Only an upper limit was obtained due to presence of a small amount of the highly emissive mononuclear ruthenium metallopeptides (**1′**). ^{e} The long-lived component is assigned to the mononuclear ruthenium metallopeptides (**1′−3′**). These constitute <3% of the total concentration of emissive species.

Synthesis of [Ruᴵᴵ(bpy)₂(4-carboxy-4′-methyl-2,2′-bipyridine)]-(PF₆)₂. The ruthenium polypyridyl complex [Ru(bpy)₂(cmbpy)](PF₆)₂ was prepared as previously described (bpy = 2,2′-bipyridine, cmbpy = 4-carboxy-4′-methyl-2,2′-bipyridine).[10b]

Synthesis of [(NH₃)₅Coᴵᴵᴵ(Val)ₙNH₂](BF₄)₃, n = 1−3. The carboxyl-protected cobalt metallopeptides were prepared using methods previously described.[28]

Synthesis of [Ruᴵᴵ(bpy)₂(4-carboxy-4′-methyl-2,2′-bipyridine)−(Val)ₙ−Coᴵᴵᴵ(NH₃)₅](TFA)₄, n = 1−3. The binuclear complexes [Ru(bpy)₂(cmbpy)−(Val)ₙ−Coᴵᴵᴵ(NH₃)₅](BF₄)₄, n = 1−3, were prepared using methods previously described for the analogous proline-bridged complexes.[10b] The binuclear Ru−Co metallopeptides were then purified by semipreparative reverse-phase HPLC (25% v/v CH₃CN/H₂O, 0.1% v/v HTFA) and identified by one-dimensional ¹H NMR: 10% D₂O/H₂O v/v, 298 K, 400 MHz.

[Ru(bpy)₂(cmbpy)−(Val)₁−Co(NH₃)₅](TFA)₄ (1): δ 8.71 (d, 1H, NH), 8.67 (s, 1H, Ar), 8.44 (d, 4H, Ar), 8.38 (s, 1H, Ar), 7.96 (t, 4H, Ar), 7.89 (d, 1H, Ar), 7.70 (m, 4H, Ar), 7.54 (dd, 2H, Ar), 7.29 (t, 4H, Ar), 7.18 (s, 1H, Ar), 4.80 (s, residual solvent), 4.29 (m, 1H, C$_\alpha$H), 3.82 (s, 12H, cis-NH₃), 2.84 (s, 3H, trans-NH₃), 2.45 (s, 3H, CH₃), 2.15 (m, 1H, C$_\beta$H), 1.00 (dd, 3H, C$_\gamma$H), 0.86 (dd, 3H, C$_\gamma$H).

[Ru(bpy)₂(cmbpy)−(Val)₂−Co(NH₃)₅](TFA)₄ (2): δ 8.89 (d, 1H, NH), 8.74 (s, 1H, Ar), 8.50 (d, 4H, Ar), 8.45 (s, 1H, Ar), 8.30 (d, 1H, NH), 8.02 (t, 4H, Ar), 7.95 (d, 1H, Ar), 7.76 (m, 4H, Ar), 7.59 (dd, 2H, Ar), 7.34 (t, 4H, Ar), 7.24 (d, 1H, Ar), 4.80 (s, residual solvent), 4.32 (m, 1H, C$_\alpha$H), 4.19 (m, 1H, C$_\alpha$H), 3.87 (s, 12H, cis-NH₃), 2.91 (s, 3H, trans-NH₃), 2.51 (s, 3H, CH₃), 2.12 (m, 2H, C$_\beta$H), 0.99 (m, 6H, C$_\gamma$H), 0.85 (m, 6H, C$_\gamma$H).

[Ru(bpy)₂(cmbpy)−(Val)₃−Co(NH₃)₅](TFA)₄ (3): δ 8.89 (d, 1H, NH), 8.74 (s, 1H, Ar), 8.50 (d, 4H, Ar), 8.46 (s, 1H, NH), 8.33 (d, 1H, Ar), 8.13 (d, 1H, NH), 8.02 (m, 4H, Ar), 7.95 (d, 1H, Ar), 7.91 (s, 2H, Ar), 7.76 (s, 2H, Ar), 7.60 (dd, 2H, Ar), 7.35 (d, 4H, Ar), 7.25 (d, 1H, Ar), 4.80 (s, residual solvent), 4.28 (m, 1H, C$_\alpha$H), 4.18 (m, 1H, C$_\alpha$H), 4.11 (m, 1H, C$_\alpha$H), 3.86 (s, 12H, cis-NH₃), 2.90 (s, 3H, trans-NH₃), 2.53 (s, 3H, CH₃), 2.13 (m, 3H, C$_\beta$H), 0.90 (m, 18H, C$_\gamma$H).

Synthesis of [Ruᴵᴵ(bpy)₂(4-carboxy-4′-methyl-2,2′-bipyridine)-(Val)ₙ](TFA)₂, n = 1−3. The mononuclear ruthenium metallopeptides (**1′−3′**) were prepared by reducing the cobalt center of the corresponding binuclear Ru−Co metallopeptide with zinc amalgam in argon-saturated 0.1 M trifluoroacetic acid (HTFA).

Results and Discussion Section

Synthesis and Characterization of the Complexes. The binuclear metallopeptides, [Ruᴵᴵ(bpy)₂(4-carboxy-4′-methyl-2,2′-

bipyridine)−(Val)ₙ−Coᴵᴵᴵ(NH₃)₅], n = 1−3 (**1−3**), were prepared by coupling the mononuclear complexes [Ru(bpy)₂-(cmbpy)]²⁺ and [(NH₃)₅Co(Val)ₙ]³⁺ by a carbodiimide reaction. The resulting compounds were purified by reverse-phase HPLC. ¹H NMR spectra obtained in D₂O (not shown) clearly show the presence of the slowly exchanging cis and trans cobalt pentaammine peaks,[29] in addition to those belonging to the valinyl peptide residues and the ruthenium polypyridyl complex. Treatment of these compounds with zinc amalgam produced the related mononuclear ruthenium metallopeptides (**1′−3′**). These compounds had significantly longer HPLC retention times than those of their parent Ru−Co species. In addition, their ¹H NMR spectra showed the absence of the Co(NH₃)₅ peaks at 3.9 and 2.9 ppm. The absorption spectra of all compounds (**1−3**, **1′−3′**) are nearly superimposable, being dominated by features arising from the [Ru(bpy)₂(cmbpy)] chromophore.[10b]

The corrected steady-state emission spectra of **1−3** and **1′−3′** consist of a broad peak whose λ_{max} falls within the range of 669 ± 4 nm in aqueous solution at 298 K (Table 1). The peak maxima are solvent dependent, becoming blue-shifted to 646 ± 2 nm in 4:1 (v/v) ethanol−methanol (298 K). The spectra obtained at 77 K in the ethanol−methanol glass show a vibrational progression of $\hbar\omega$ (119−142) × 10³ cm⁻¹ similar to that seen for other polypyridyl ruthenium(II) compounds (data not shown).[30] A similar solvent dependence of λ_{max} in fluid solution was recently observed for [Ru(bpy)₂(3,5-dicarboxy-2,2′-bipyridine)], which results from strong solute−solvent interactions involving the substituted bipyridine. Interestingly, this situation results in an emission lifetime that increases with increasing temperature in aqueous solution.[31]

Conformational Properties of 1−3. The partial-double-bond character of amide bonds enables the backbone conformations of polypeptides to be determined by the torsion angles ϕ and ψ. ¹H NMR experiments can therefore be used to help deduce their three-dimensional structures. The Karplus relationships have been used to show that the amino acids found within

(28) Isied, S. S.; Vassilian, A. *J. Am. Chem. Soc.* **1984**, *106*, 1732.

(29) Mobashar, R. M.; Taylor, A., Jr.; Marzilli, L. G. *Inorg. Chim. Acta* **1991**, *186*, 139.

(30) Hager, G. D.; Crosby, G. A. *J. Am. Chem. Soc.* **1975**, *97*, 7031.

(31) (a) Fernando, S. R. L.; Maharoof, U. S. M.; Deshayes, K. D.; Kinstle, T. H.; Ogawa, M. Y. *J. Am. Chem. Soc.* **1996**, *118*, 5783. (b) Fernando, S. R. L.; Ogawa, M. Y. *Chem. Commun.* **1996**, 637.

Table 2. ¹H NMR Parameters for **1−3** in H_2O/D_2O (9:1 v/v) at 298 K

residue	**1**	**2**[a]		**3**[b]		
	A	A	B	A	B	C
δ_{298K} (ppm)	8.66	8.89	8.31	8.92	8.48	8.12
$^3J_{NH-C_\alpha H}$ (Hz)	8.0	7.4	8.0	6.9	8.0	8.6

[a] Strong NOESY cross-peaks are seen between NH_B and $C_\alpha H_A$. [b] Strong NOESY cross-peaks are seen between NH_C and $C_\alpha H_B$ and between NH_B and $C_\alpha H_A$.

the β-sheet structure should display a combination of $\phi = -139°$ and $\psi = +135°$ which give large values of $^3J_{NH-C_\alpha H}$ (>7.5 Hz) and strong sequential $(i, i + 1)$ $NH-C_\alpha H$ NOESY cross-peaks.[27]

The NMR properties of the Ru−Co metallopeptides (**1−3**) are shown in Table 2. Evidence for the β-strand structure can be found within the values of $^3J_{NH-C_\alpha H}$ observed for the amide protons in these compounds, except the ones positioned closest to the bipyridyl ligand in **2** and **3**. Computer models show that steric interactions involving the H3 and H5 positions of the bipyridine ring are the probable cause of this deviation. Interestingly, the coupling constant for the single valine residue of **1** does not show this deviation $(^3J_{NH-C_\alpha H} = 8$ Hz), which suggests that additional interactions involving the now proximal $Co(NH_3)_5$ site serve to enforce the β-strand conformation of the monopeptide. Thus, the single-residue metallopeptide, **1**, appears to display an unexpectedly large degree of conformational rigidity. Examination of the 2D NOESY spectra of **2** and **3** provide additional evidence for the β-strand conformation as strong sequential NOESY cross-peaks are observed. Thus, on the NMR time scale, the Ru−Co metallopeptides are shown to possess the conformational properties inherent within the individual peptide strands of a β-pleated sheet. To further examine the conformational homogeneity of the samples, emission lifetime measurements were performed on the binuclear electron-transfer compounds **1−3** in a frozen alcohol glass at 77 K. Under these conditions, it is expected that quench cooling of an equilibrium population of interconverting conformations in fluid solution should produce a static distribution of the individual conformations in the cryogenic glass. As will be discussed below, the quenched emission of each of these compounds follows single-exponential electron-transfer kinetics, which implies that these species maintain a unique donor/acceptor separation and do *not* exist within a equilibrium distribution of conformations at 298 K.

Emission Lifetimes of the Mononuclear Ruthenium Metallopeptides (1′−3′). Emission lifetime measurements were performed on the mononuclear ruthenium peptides (**1′−3′**) at 298 K in aqueous solution and 4:1 ethanol−methanol and at 77 K in the alcohol glass. In all cases, the emission decay followed simple first-order kinetics (eq 4), where τ_0 is the

$$I_{em}(t) = A_0 \exp(-t/\tau_0) \qquad (4)$$

emission lifetime $(\tau_0 = 1/k_0)$ and A_0 is the maximum emission amplitude produced by the laser flash. As seen in Table 1, the emission lifetimes at 298 K are strongly solvent dependent, with the shorter lifetimes being observed in water. Similar behavior has been reported for related ruthenium polypyridyl compounds.[31,32]
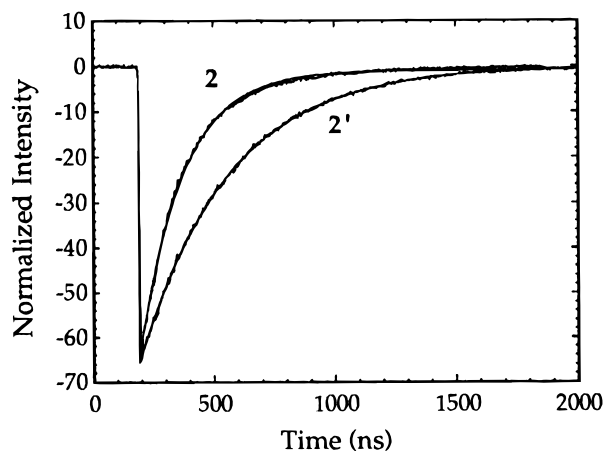
(32) (a) Juris, A.; Balzani, V.; Barigelletti, F.; Campagna, S.; Belser, P.; Von Zelewsky, A. *Coord. Chem. Rev.* **1988**, *84*, 85. (b) Meyer, T. J. *Pure Appl. Chem.* **1986**, *58*, 1193.

Figure 2. Emission decay curves of **2** and **2′** in aqueous solution at 298 K showing a shortened lifetime for the binuclear donor/acceptor compound. The subtle deviation from the fit to single-exponential behavior (eq 4) seen for **2** at longer times is assigned to the presence of mononuclear ruthenium impurities as described in the text.

Emission Lifetimes of the Binuclear Metallopeptides (1−3). Emission lifetime measurements were performed on multiple samples of the binuclear ruthenium−cobalt peptides (Table 1). When **3** was dissolved in aqueous solution (298 K), its emission followed a single-exponential decay which could be accurately fit to eq 4 to yield a value of $\tau = 290 \pm 12$ ns. This lifetime is distinctly shorter than that of its analogous mononuclear peptide, **3′**. Freshly prepared samples of the smaller binuclear peptides **1** and **2** also showed faster emission decays than those of their parent ruthenium peptides (Figure 2). However, whereas the decay of freshly prepared samples of **2** could be fit to single-exponential kinetics, evidence for a longer-lived emission could often be seen in older samples. The decay of **1** was always distinctly biexponential. Prolonged exposure of both of these solutions to light resulted in the continued growth of the longer-lived emission component, indicating the existence of a photoinduced electron-transfer process (vide infra). Once the amplitude of this new emission was sufficiently large (>10% of the total emission), the resulting decay profiles could be accurately fit to eq 5, where τ_S and τ_L are respectively

$$I_{em}(t) = A_S \exp(-t/\tau_S) + A_L \exp(-t/\tau_L) \qquad (5)$$

the short and long emission lifetime components and A_S and A_L are their relative amplitudes. Use of this treatment resulted in values of $\tau_S < 10$ ns and $\tau_L = 380 \pm 10$ ns for **1** and $\tau_S = 123 \pm 20$ ns and $\tau_L = 373 \pm 6$ ns for **2**. Since an accurate value for τ_S could not be obtained for **1** using the nanosecond laser apparatus, picosecond phase-shift fluorimetry was used to obtain a value of $\tau_S = 0.5 \pm 0.3$ ns. The similarity in the values of τ_L and the lifetimes of the related ruthenium peptides, **1′** and **2′**, allows their assignment to the presence of mononuclear ruthenium polypeptide impurities. The values of A_L and A_S were used to determine the relative molar concentrations of the short- and long-lived emission species by using the magnitude of τ as a measure of the emission quantum yield. For freshly prepared solutions of **1−3**, the long-lived component comprises less than 3% of the total molar concentration of emissive species. The very large difference in the values of τ_L and τ_S, and thus in ϕ_L and ϕ_S, causes the emission properties of **1** and **2** to be very sensitive to the presence of even small amounts of long-lived impurities in aqueous solution.
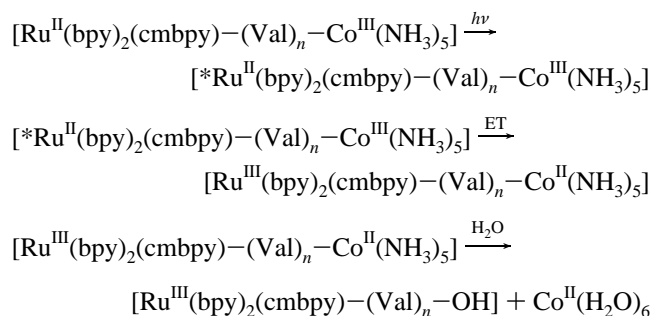
The emission decays of **1−3** follow biexponential kinetics in 4:1 (v/v) ethanol−methanol at 298 K. For all three

compounds, fits of the data to eq 5 yield values of $\tau_L \approx 1100$ ns, which can be again assigned to the presence of mononuclear ruthenium impurities. The observation of biexponential behavior in this solvent results from the enhanced quantum yield of the impurity as indicated by the increased value of τ_L in ethanol–methanol. Analysis of these data indicate that the molar concentration of the longer emitting species is still <3% of the total amount of ruthenium species present in these solutions. As will be discussed below in more detail, we note that the lifetime (τ_S) of the predominant, short-lived species increases with increasing chain length: $\tau_S < 0.5$ ns for **1**, $\tau_S = 77 \pm 8$ ns for **2**, and $\tau_S = 220 \pm 30$ ns for **3** (Table 1). It is further noted that, at 77 K, the emission decays of **2** and **3** could be accurately fit to a single-exponential decay for which $\tau = 2620 \pm 250$ ns and $\tau = 4250 \pm 300$ ns, respectively. However, the decay of **1** is biexponential with $\tau_S = 10 \pm 4$ ns and $\tau_L = 4850 \pm 100$ ns which again results from the presence of a small amount of ruthenium impurity. The observation of a single quenched emission lifetime for each of the binuclear compounds in the frozen glass indicates that these compounds maintain a unique donor/acceptor separation.

Mechanism for Emission Quenching in 1−3. Under all conditions studied, the emission lifetimes of the binuclear metallopeptides (**1−3**) are shorter than those of the mononuclear analogues (**1′−3′**). These results are consistent with Scheme 1, which involves photoinduced electron transfer to the Co(III)

Scheme 1

$$[Ru^{II}(bpy)_2(cmbpy)-(Val)_n-Co^{III}(NH_3)_5] \xrightarrow{h\nu}$$
$$[*Ru^{II}(bpy)_2(cmbpy)-(Val)_n-Co^{III}(NH_3)_5]$$

$$[*Ru^{II}(bpy)_2(cmbpy)-(Val)_n-Co^{III}(NH_3)_5] \xrightarrow{ET}$$
$$[Ru^{III}(bpy)_2(cmbpy)-(Val)_n-Co^{II}(NH_3)_5]$$

$$[Ru^{III}(bpy)_2(cmbpy)-(Val)_n-Co^{II}(NH_3)_5] \xrightarrow{H_2O}$$
$$[Ru^{III}(bpy)_2(cmbpy)-(Val)_n-OH] + Co^{II}(H_2O)_6$$

acceptor followed by aquation of the reduced cobalt site. A similar mechanism has been reported for the excited-state quenching of Ru(bpy)$_3^{2+}$ by various (carboxylato)pentamminecobalt(III) complexes.[33] To determine that this mechanism also obtains in the present situation, a sample of **1** was subjected to multiple laser pulses until the emission decay could be fit to single-exponential behavior having a long lifetime ($\tau = 388 \pm 8$ ns) which is identical to that of the mononuclear ruthenium peptide. Reverse-phase HPLC of the photolyzed solution showed the appearance of a new ruthenium polypyridyl product having the same retention time as **1′**. No evidence for the Ru−Co peptide was observed. On the basis of these experiments, we assign the quenching process in **1−3** to a photoinduced electron-transfer event. However, an accompanying energy-transfer mechanism cannot be ruled out at this time.

The rate constants for electron transfer (k_{et}) can be calculated according to eq 6 where τ_{obs} is the concentration independent

$$k_{et} = \tau_{obs}^{-1} - \tau_0^{-1} \tag{6}$$

emission lifetime of the binuclear metallopeptide and τ_0 is the lifetime of the appropriate mononuclear model compound. The data presented in Table 1 show the expected trend of decreasing
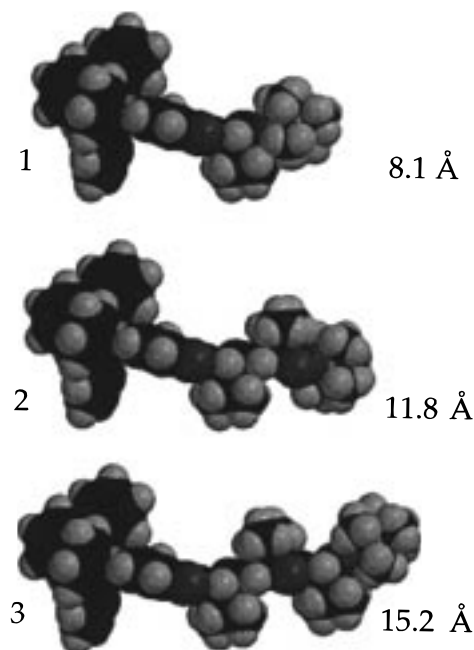
(33) Bottcher, W.; Haim, A. *J. Am. Chem. Soc.* **1980**, *102*, 1564.

Figure 3. Energy-minimized conformations of **1−3** using the SYBIL force field. The resulting values of ϕ and ψ are consistent with those obtained from the NMR data.

values of k_{et} with increasing donor/acceptor separation, as will be discussed in the next section. In addition, the data also show that the ET rates obtained in the ethanol–methanol glass at 77 K are 2 orders of magnitude smaller than those obtained in the same solvent at 298 K. It is of interest to note that these systems are seen to undergo photoinduced electron transfers at cryogenic temperatures despite their relatively modest driving force. Recent work by several groups[34] has shown that the driving force for ET reactions occurring in rigid media is significantly lower as compared to that in fluid solution due to the reduced solvent stabilization of the product ion pair. It appears that this effect is less pronounced in the present charge-shift reaction.

Distance Attenuation of k_{et}. Molecular modeling studies were used to estimate the donor/acceptor separations in **1−3** in which the energy-minimized structures displayed values of ϕ and ψ which were in good agreement with those obtained from the NMR data. On the basis of these results, the through-space, edge-to-metal distances (d_{E-M}) separating the ruthenium polypyridyl and cobalt pentaammine sites are 8.1, 11.8, and 15.2 Å for **1−3**, respectively (Figure 3). A plot of $\ln k_{et}$ vs d_{E-M} for the data obtained in H$_2$O at 298 K and in the ethanol–methanol glass at 77 K is shown in Figure 4. The data obtained in the fluid alcohol solution are not plotted but can be seen in Table 1.

The three data points obtained in fluid aqueous solution appear to deviate somewhat from the exponential distance dependence expected for long-range donor/acceptor interactions (eq 3). This behavior is somewhat reminiscent of the nonexponential distance dependence previously reported for a series of proline-bridged donor/acceptor compounds.[10] However, at this point, it is not clear if the same effect is being observed. A fit of our data to eq 3 yields $\beta = 1.1 \pm 0.4$ Å^{-1} where, in this case β is an empirical distance attenuation factor which contains contributions from *both* the electronic and nuclear terms of eq

(34) (a) Chen, P.; Meyer, T. J. *Inorg. Chem.* **1996**, *35*, 5520. (b) Harriman, A.; Heitz, V.; Ebersole, M.; van Willigen, H. *J. Phys. Chem.* **1994**, *98*, 4982. (c) Gaines, G. L., III; O'Neil, M. P.; Svec, W. A.; Niemczyk, M. P.; Wasielewski, M. R. *J. Am. Chem. Soc.* **1991**, *113*, 719.
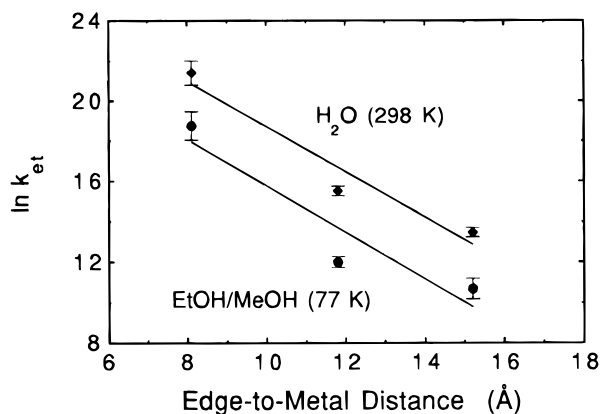
Figure 4. Plot of ln k_{et} vs d_{E-M} for **1**−**3** at 298 K in aqueous solution and at 77 K in 4:1 (v/v) ethanol−methanol. For both cases, a fit of the data to eq 3 yields a value of $\beta = 1.1 \pm 0.4$ Å^{-1}. The error bars reflect the standard deviation obtained from measuring multiple samples of each compound.

1. It is thus possible that the apparent curvature in the ln k_{et} vs distance plot may be due to contributions arising from the distance dependence of the solvent reorganization term. However, use of the Marcus two-sphere model to calculate the solvent reorganization energy was unable to improve the quality of the fit. This treatment also appears to overestimate the activation barrier for electron transfer as the resulting values for activationless ET rates ($k_{max} = k_{obs} \exp(\Delta G^*/RT)$) extrapolate to an unreasonably large value of k_{max} at the donor/acceptor contact distance (ca. 10^{19} s^{-1}). Interestingly, the observation of a small solvent contribution to the reorganization energy is consistent with the kinetic data obtained in the alcohol glass at 77 K, which show a distance dependence of k_{et} that is nearly identical to that observed in fluid aqueous solution (Figure 4). It is interesting to note that a systematic change in electron-transfer rates can be seen for each compound when measured in the fluid solution vs the rigid glass. The similarity in behavior observed under such different solvent conditions suggests that outer-sphere reorganization plays only a modest role in governing the distance dependence of ET rates in these systems. This is especially true for the data obtained at 77 K, where the high-frequency contributions to the FCWD term can be reasonably assumed to be absent. Such behavior appears to be in marked contrast to that seen for a related series of proline-bridged donor/acceptor compounds in which solvent reorganization dominates the distance dependence of k_{et}.[18]

In summary, the distance dependence of electron-transfer rates has been observed for compounds **1**−**3** both in fluid aqueous solution and in a low-temperature alcohol glass. In both cases, an empirical distance attenuation factor of $\beta = 1.1 \pm 0.4$ Å^{-1} is observed in which the effects of solvent reorganization are apparently small. At this point, it is tempting to compare the distance dependence of k_{et} observed here with that seen for ET reactions occurring along the β-strands of ruthenium-modified azurin ($\beta = 1.1$ Å^{-1})[35] and the range predicted by Gray and co-workers for ET occurring along an individual strand of a β-pleated sheet ($\beta = 0.9-1.15$ Å^{-1}).[36] However, the large uncertainty in the fit of our data to eq 3 is cause for additional study. The results of the emission lifetime measurements made at 77 K and the solution-phase NMR at 298 K argue against the existence of conformational equilibria as being a potential source of this problem. Similarly, the apparent nonexponential distance dependence at 298 K cannot be explained by correcting for outer-sphere reorganization energy using the dielectric continuum model. This appears to be consistent with the quite similar distance dependence observed in the low-temperature glass. Thus, to further understand the nature of the distance dependence of ET rates in synthetic β-strands, we are presently studying the properties of an analogous series of compounds in which there is a larger driving force for electron transfer and for which the electron-transfer event can be directly observed by transient absorption spectroscopy.

(35) Langen, R.; Chang, I.-J.; Germanas, J. P.; Richards, J. H.; Winkler, J. R.; Gray, H. B. *Science* **1995**, *268*, 1733.
(36) Gray, H. B.; Winkler, J. R. *Annu. Rev. Biochem.* **1996**, *65*, 537.